Carderock Division
Naval Surface Warfare Center
Bethesda, Maryland 20084-5000

CARDIVNSWC-TR-61-94/28 November 1994
Metals and Welding Department
Research and Development Report

Static Recrystallization Behavior of Austenite in HSLA 100 During Thermomechanical Controlled Processing (TMCP)

by
E.M. Focht

CARDIVNSWC-TR-61-94/28 Static Recrystallization Behavior of Austenite in HSLA 100 During Thermomechanical Controlled Processing (TMCP)

Carderock Division
Naval Surface Warfare Center
Bethesda, Maryland 20084-5000

CARDIVNSWC-TR-61-94/28 November 1994
Metals and Welding Department
Research and Development Report

Static Recrystallization Behavior of HSLA 100 During Thermomechanical Controlled Processing (TMCP)

by
E.M. Focht

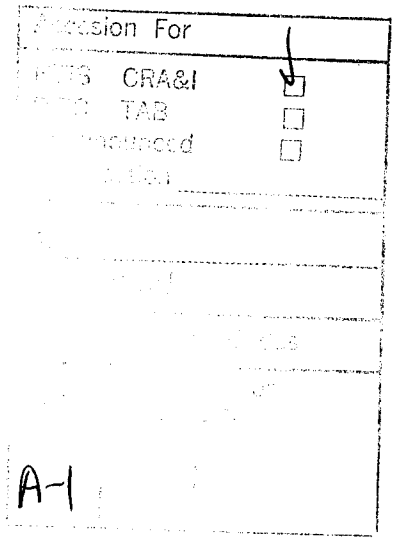

CONTENTS

ABSTRACT 1

ACKNOWLEDGEMENTS 1

ADMINISTRATIVE INFORMATION 1

INTRODUCTION 2

EXPERIMENTAL PROCEDURE 4
MATERIALS 4
METHODS 4

RESULTS 6

DISCUSSION 7

CONCLUSIONS 12

REFERENCES 13

TABLES

Table 1 Chemical Composition of HSLA-100 Slab Material 17

Table 2 Dissolution Temperatures of Various Carbonitride Precipitate Species Based On Equilibrium Solubility Equations [Palmeire, 1994] 17

FIGURES

Figure 1 The three stages of thermomechanical processing [Tanaka, 1984] 18

Figure 2 Schematic illustration of true stress/true strain curves obtained to measure static softening during multi-hit deformation tests. 18

Figure 3 Microstructure of HSLA-100 in the as-slabbed condition. 19

Figure 4 Schematic illustration of the TMCP specimen. 19

Figure 5 Schematic illustration of processing routes for (a) the recrystallization study and (b) the RCR and RCR + CR simulations. 20

Figure 6 (a) Fractional softening vs. hold time for HSLA-100 deformed at 900°C (1650°F) and 10% deformation, and (b) the corresponding true stress/true strain curves for the 60 second hold time. 21

Figure 7 (a) Fractional softening vs. hold time for HSLA-100 deformed at 900°C (1650°F) and 20% deformation, and (b) the corresponding true stress/true strain curves for the 60 second hold time. 22

Figure 8 (a) Fractional softening vs. hold time for HSLA-100 deformed at 982°C (1800°F) and 10% deformation, and (b) the corresponding true stress/true strain curves for the 60 second hold time. 23

Figure 9 (a) Fractional softening vs. hold time for HSLA-100 deformed at 982°C (1800°F) and 20% deformation, and (b) the corresponding true stress/true strain curves for the 20 second hold time. 24

Figure 10 Microstructures of HSLA-100 subjected to (a-d) RCR processing at 1800°F (982°C) and different hold times, strains and number of hits and (e) RCR at 1800°F (982°C) + CR at 1550°F (982°C). 25

Figure 11 The softening behavior of various (a) Nb steels and (b) Ti steels with 0.002% C. These curves illustrate the effect of Nb and Ti in solution in austenite at the deformation temperature. [Yamamoto et al. 1982] 28

Figure 12 Isothermal precipitation of Nb in undeformed austenite in a 0.07% C, 0.04% Nb, 0.01% N steel. [Simoneau et al., 1978] 29

Figure 13 Influence of strain level on the kinetics of Nb precipitation at 900°C (1650°F). [DeArdo, 1984] 29

Figure 14 Recrystallization-precipitation diagram for C-Mn and C-Mn-Nb steels. [Yamamoto et al., 1982] 30

Figure 15 Grain growth behavior after hot rolling (a) Si-Mn steel (b) Nb steel and (c) Ti steel. [Ouchi et al., 1976] 31

Figure 16 Effect of interpass time and deformation temperature on the softening ratio: Si-Mn steel, prestrain 0.2. [Ouchi et al., 1988] 32

Figure 17 Fraction of softening vs true strain for deformation tests performed at 1650°F (900°C) with (a) 10% deformation per hit and (b) 20% deformation per hit. 33

Figure 18 Fraction of softening vs true strain for deformation tests performed at 1800°F (982°C) with (a) 10% deformation per hit and (b) 20% deformation per hit. 34

ABSTRACT

The austenite recrystallization behavior during the hot deformation of HSLA-100 was characterized in order to determine parameters for thermomechanical controlled processing. The steel was reheated to 2000°F (1093°C) and subjected to multiple isothermal deformations at 1800°F (982°C) and 1650°F (900°C) under various levels of deformation and hold times. At 10% deformation per hit, the steel took longer than 20 seconds to recrystallize at 1800°F (982°C) after three hits while at 1650°F (900°C) the steel did not recrystallize during the hold periods. At 20% deformation per hit, the steel began to recrystallize after the first hit after 20 seconds and recrystallized repeatedly after each subsequent hit during all of the hold periods at 1800°F (982°F) while at 1650°F (900°C), recrystallization occurred after three hits and the 20 second hold time. The retardation of static recrystallization was attributed to the pinning effect of niobium carbonitride species that precipitated at austenite grain boundaries and subgrains following deformation. The information gained from the recrystallization study was used to successfully perform recrystallization controlled rolling (RCR) and recrystallization controlled rolling plus controlled rolling (CR) simulations.

ACKNOWLEDGEMENTS

The author would like to acknowledge Ms. L.R. Link (formerly with CDNSWC, Code 614), Mr. S. V. Womack (Code 614) and Dr. M.G. Vassilaros (Code 615) for their assistance over the course of this project. Mr. A. Brandemarte performed the quantitative metallography in this study.

ADMINISTRATIVE INFORMATION

This report was prepared as part of the Ship and Submarine Materials Technology Program sponsored by ONR 332 (Dr. Lewis Sloter). Mr. Ivan Caplan of the Carderock Division, Naval Surface Warfare Center (CDNSWC Code 0115) is the Technology Area Manager for this program. This effort was performed by the Fatigue and Fracture Branch, CDNSWC Code 614 under Program

Element 62234N, Structural Alloys Project RS34S55, Work Unit 1-6140-502, and was supervised by the Branch Head, Mr. T.W. Montemarano.

INTRODUCTION

Thermomechanical controlled processing (TMCP) of HSLA steels was developed to achieve high strengths and toughnesses at very low alloying levels. There are four stages of TMCP -- Stage 1: Deformation above the austenite recrystallization temperature; Stage 2: Deformation below the austenite recrystallization temperature; Stage 3: Deformation in the two-phase ($\alpha + \gamma$) region; and Stage 4: Accelerated cooling [Tanaka, 1984]. Stage 1 is often referred to as the recrystallization controlled rolling, or RCR, regime and Stage 2 the controlled rolling, or CR, regime. The temperature of demarcation between the two regions is the recrystallization stop temperature, T_{rxn}. When the steel is rolled above the T_{rxn}, the austenite recrystallizes during the hold time between passes; however, when the steel is rolled below T_{rxn}, the austenite does not recrystallize during the hold period. The prior austenitic microstructure that results from processing in the RCR and CR regimes are different in that RCR processing produces an equiaxed austenite grain morphology while CR produces a flattened or pancaked austenitic structure. Figure 1 is a schematic diagram showing the three stages of controlled rolling and some of the possible austenitic and transformed microstructures. The desired condition of the austenite prior to cooling will depend on the mechanical properties required of the steel. To achieve both high strength and high toughness, controlled rolling is used to achieve a fine pancaked prior austenite grain structure containing a large volume of substructure within the grains that result in a very fine transformation product of either ferrite, ferrite and bainite, bainite and martensite or martensite [DeArdo, 1988(b)]. RCR is an effective means of obtaining a refined equiaxed austenitic grain size compared to hot rolling. High strengths and good toughnesses are achievable via RCR, but to a lesser degree than those attainable via CR; the difference lies in the higher amount of grain refinement that results from CR. RCR is often used to condition the austenite prior to CR as opposed to hot rolling before CR.

In order to prescribe a specific TMCP route, T_{rxn} must be determined. Therefore, the recrystallization kinetics must be characterized as a function of processing parameters such as the

deformation temperature, strain and hold time between passes. The method of hot compression has been used successfully to characterize the effect of processing on austenite recrystallization [Djaic and Jonas, 1973, Luton, et al, 1980, Yamamoto, et al, 1982, and Yoshie, et al, 1987, Kwon and DeArdo, 1991]. The method of hot compression or double deformation, as it may be called, is performed by heating the steel to a slab reheat temperature, cooling to the deformation temperature, deforming to a certain strain followed immediately by unloading, holding at temperature for a precise hold time and then deforming the specimen again. Load and displacement are recorded as a function of time and later converted to true stress vs true axial strain. In deformation studies, the deformation step is often referred to as a "hit" and is analogous to a rolling "pass." The term "hit" is used here to refer to the deformation step in the process simulations.

It is the interpretation of the hot flow behavior that gives insight into recrystallization kinetics. As the steel begins to strain-harden during deformation, dislocations are created. During the hold period the dislocation density will decrease and the hot strength of the steel will consequently decrease (i.e. the steel will soften) if recovery and/or recrystallization occur. As a result, the flow stress of the second hit will be lower than the peak stress of the first hit. The fraction of softening that takes place between hits may be determined using the following relation:

$$X_s = \frac{\sigma_m - \sigma_{off}}{\sigma_m - \sigma_0} \qquad [1]$$

where σ_m is the peak stress after the first hit, and σ_0 and σ_{off} are the offset yield stresses of the first and second hits, respectively. Figure 2 is a schematic diagram of true stress/true strain curves indicating the parameters defined in Eq. [1]. When X_s is plotted against the hold time with the hold time on a log scale, the shape of the curve is usually sigmoidal. The onset of recrystallization has been reported to correspond to about 0.20 fractional softening [Yamamoto et al., 1982]. Any softening below 0.20 is attributed to recovery processes.

The double deformation technique provides valuable information on the kinetics of austenite recrystallization following a single pass. However, single pass kinetics do not give insight into the

effects of retained strain following severe deformation below the apparent T_{nr} following several passes. Past work incorporating several passes in the rolling simulations has been performed while the temperature of the specimen was continuously decreasing from the reheat temperature to the final rolling temperature with a ΔT from 600 - 1188°F (300 - 600°C) [Barbosa et al., 1988, and Cuddy et al., 1980]. However, modern controlled rolling practices sometimes requires several rolling passes to be performed within a temperature window of only 18°F (10°C). Therefore, isothermal compression testing utilizing more than one pass should provide valuable information regarding the effects of retained strain on the kinetics of austenite recrystallization.

The objective of this study was to characterize the static recrystallization behavior of HSLA-100 steel containing niobium and titanium as microalloying elements. Multi-hit deformation simulations were conducted by adopting the methodology of double deformation testing. The information gained in the study was used to perform TMCP simulations to determine the effects of various processing parameters on the mechanical properties of HSLA-100 and is the subject of a future report.

EXPERIMENTAL PROCEDURE

MATERIALS

HSLA-100 with the composition shown in Table 1 was provided as a twelve inch thick slab with a reported ASTM grain size number between 7-8. The microstructure of the slab is shown in Figure 3 and appears to be consistent with the microstructures found in 0.04% C HSLA-100 [Wilson et al., 1988, Hamberg and Wilson, 1988]. In thick sections, the slow cooling frequently results in a microstructure consisting of particles of retained austenite, martensite and carbides embedded in a matrix of ferrite with an acicular morphology. This microstructure is sometimes referred to as "granular bainite" [Thompson, et al. 1990]. The exact nature of the microstructural constituents present in the slab is uncertain because they were not identified by electron microscopy.

METHODS

The TMCP simulator consisted of a 500 kip MTS servohydraulic test machine integrated with

10 kW induction heater. The MTS machine is controlled with an MTS Model 418.91 Microprofiler. Load, time and displacement data were acquired using a Nicolet System 500 digital acquisition system and were converted to true stress and true axial strain values.

Specimens for TMCP simulations were machined from the slab material and had a geometry as shown in Figure 4. Graphite impregnated paper and a glass frit (Deltaglaze 349) were used as lubricants. Each specimen was heated to the reheat temperature, held for five minutes, and then cooled to the deformation temperature. After holding at the deformation temperature for one minute, the specimen was subjected to four hits total and held for the desired hold time between each hit. The processing schedule is shown diagrammatically in Figure 5(a). A slab reheat temperature of 2000°F (1093°C) was chosen to ensure the dissolution of the niobium carbonitrides and to limit grain growth. The deformation temperatures of 1800°F (982°C) and 1650°F (900°C) were chosen to determine the temperature ranges and deformation parameters for recrystallization controlled rolling and controlled rolling, respectively. The percent deformations of 10% and 20% and the hold times of 2, 5, 20, and 60 seconds are typical ranges for these parameters used in the TMCP of steels.

The softening behavior of the steel was analyzed by applying Eq. [1] to the flow curves of all four hits. The softening that took place during the hold period after the first hit was measured using the standard technique set forth for double deformation tests and is described in a previous section of this report. When measuring the level of softening that took place during the hold periods after the second and third hits, it first had to be determined whether or not recrystallization had occurred during the previous hold period. If recrystallization did *not* occur during the previous hold period, the σ_o in Eq. [1] of the first hit was used instead of the σ_o of the previous hit. If recrystallization did occur during the previous hold period, the σ_o of the flow curve of the hit prior to the current hold period was used. The σ_m of the previous hit was used in all cases, regardless of whether or not recrystallization took place during the previous hold period.

Since RCR and a combination of RCR plus CR were going to be performed in future studies, specimens were subjected to the processing schedules shown schematically in Figure 5(b) to determine the parameters necessary to yield a recrystallized austenitic microstructure for RCR and a pancaked austenitic microstructure for RCR plus CR. For metallographic examination the prior

austenite grain boundaries were decorated with precipitates by tempering the specimens at 1100°F (593°C) for 24 hours. The polished specimens were etched in a solution of saturated picric acid and 1 wt.% dodecylbenzenesulfonic acid sodium salt (a wetting agent).

RESULTS

The load and displacement data acquired during the experiments were converted to true stress and true axial strain and analyzed graphically to measure the fraction of softening (X_s) that took place between hits. The fraction of softening was then plotted against the hold times for each test temperature. Figure 6(a) shows the softening behavior at 1650°F (900°C) where it can be seen that recrystallization did not take place for any of the hold times when the reductions are kept below 10%. However, Figure 7(a) shows that at 20% reductions, recrystallization began after three hits and a hold time of 60 seconds. Figures 6(b) and 7(b) show the true stress/true strain curves for the 60 second hold times for the 10% and 20% reductions, respectively. The degree of softening after the third hit was greater for the 20% reduction than the 10% reduction. It should also be noted that dynamic recrystallization was not evident from the stress/strain behavior. The small amount of softening occurring after the first and second hits was most likely due to static recovery.

Figures 8(a) and 9(a) show the fractional softening vs. hold times for tests performed at 1800°F (982°C) for 10% and 20% reductions, respectively. In Figure 8(a), static recrystallization is suppressed at all hold times after the first and second hits for 10% reductions. After the third hit, the steel began to recrystallize beyond the 20 second hold time and recrystallized almost completely after 60 seconds. In Figure 9(a), after the first hit, the steel began to recrystallize after about 30 seconds, within 4 seconds after the second hit and within 2 seconds after the third hit. The fraction of softening appears to level off at the 20 second hold time after the second hit. Figures 8(b) and 9(b) are true stress/true strain curves that show the softening that occurs during the hold times for tests performed at 1800°F (982°C) using 10% reductions with a 60 second hold time and 20% reductions with a 20 second hold time, respectively.

Based on the results of the recrystallization study, with hold times of 20 seconds and reductions of 20%, the T_{rxn} for this composition was determined to be 1650°F (900°C). Thus, the

processing schedules shown in Figure 5(b) were carried out to simulate RCR and RCR + CR. Figure 10 shows the microstructures and the grain sizes (ASTM E112-88) resulting from the RCR processing after three and six hits using 20% reductions and hold times of 5 and 20 seconds. The microstructures of the specimens subjected to three hits are shown in Figures 10(a) and 10(b). Un-recrystallized austenite grains are more prevalent in the specimen with the 5 second hold times than in the specimen with the 20 second hold times. However, the longer hold times resulted in a slightly larger grain size. Figures 10(c) and 10(d) show the microstructures of the specimens subjected to six hits. The austenite in these microstructures is fully recrystallized, but the average grain sizes were approximately equal to those measured in the specimens subjected to three hits, at the respective hold times. (It should be noted that Figure 10(a) is not representative of the whole microstructure but is shown here to illustrate the appearance of un-recrystallized grains.) The limited amount of un-recrystallized grains did not seem to significantly affect the average grain size. The convergence of the austenitic grain sizes to a value of around 20 μm during RCR is consistent with multipass rolling experiments performed by Sekine and Maruyama [1973] who observed a limit in the amount of austenitic grain refinement achievable when deforming above the T_{rxn}. Figure 10(e) is a photomicrograph of a specimen subjected to RCR at 1800°F (982°C) and CR at 1550°F (843°C). The pancaked austenite shown in the microstructure is indicative of austenite rolling below the T_{rxn}.

DISCUSSION

The static recrystallization behavior of low carbon steels with niobium and titanium additions has been studied extensively [Hansen et al., 1980, Luton et al., 1980, Yamamoto, et al., 1982, Barbosa, et al., 1988, Kwon et al., 1991, and Laasraoui et al., 1991]. Many of the studies incorporate isothermal single or double hit compression testing to characterize the recrystallization kinetics of austenite. However, there is little information regarding austenite recrystallization kinetics following multiple passes. As mentioned previously, both the single and double hit compression tests only measure the kinetics following the first hit. The results of the multiple hit compression tests performed here provide information regarding the effect of strain retained in the material following deformation on the recrystallization kinetics of microalloyed austenite.

The chemical composition of the austenite at the deformation temperature has been shown to significantly influence the static recrystallization kinetics of microalloyed austenite. With regards to niobium and titanium additions, niobium retards recrystallization better than titanium. Two mechanisms have been identified to explain niobium's retarding effect: solute drag and grain boundary pinning, and they depend on whether or not the microalloying elements are in solution in austenite or are in the form of precipitates, respectively. Yamamoto, et al [1982] have shown that if the microalloying elements are in solution, they retard recovery and the onset of recrystallization of deformed austenite by means of solute drag effects. They also demonstrated that the onset and the progress of static recrystallization can be delayed by the pinning of austenite grain boundaries by carbonitride precipitates (eg. Nb(CN)). Figure 11(a) is taken from the work of Yamamoto, et al. and depicts the effect of niobium in solution on the softening behavior of a 0.002% C - 0.002% N steel and shows how increased levels of niobium in solution delays the onset of recrystallization. For comparison, Figure 11(b), also from Yamamoto, et al., shows how solute titanium effects the softening behavior of a 0.002% C - 0.002% N steel. Solute niobium is clearly more effective than solute titanium at retarding recrystallization. Yamamoto, et al. [1982], isolated solute effects by severely decreasing the potential for precipitation by decarburizing the steels to 0.002 wt.% C. However, at carbon and nitrogen levels typical of HSLA steels (0.02-0.10 wt% C, <0.009% N), precipitation of microalloy carbonitrides may occur upon cooling from the slab reheat temperature. Precipitation in undeformed austenite above 1650°F (900°C) has been shown to be sluggish, as depicted in Figure 12 [Simoneau, 1978]. However, precipitation kinetics are increased markedly following deformation of the austenite. Figure 13 shows the influence of strain on the kinetics of niobium precipitation in a 0.17% C - 0.04% Nb - 0.011% N steel deformed at 1650°F (900°C). When considering the 50% precipitation time, it can be seen that 67% strain increased the kinetics by about three orders of magnitude. Superimposing precipitation kinetics data onto recrystallization kinetics data, such as in Figure 14, shows that the onset of the retardation of static recrystallization following hot deformation can be linked to the strain induced precipitation of Nb(CN).

The formation of strain induced Nb(CN) precipitates occurs at austenite grain boundaries and subgrain boundaries [DeArdo, 1988(a)]. In order to suppress recrystallization, grain boundary

mobility must be inhibited. Thus, the candidate pinning agent must exert a pinning force in excess of the driving force for static recrystallization. Calculations of the local pinning forces [Kwon, 1985 and Kwon and DeArdo, 1986] has shown that under certain conditions Nb(CN) precipitates provide sufficient resistance to pin austenite grain boundaries that otherwise would be mobile.

In addition to slowing recrystallization kinetics, Nb(CN) are also effective at inhibiting grain growth immediately following recrystallization [DeArdo, 1984]. In Figure 15, the grain growth kinetics are depicted as a function of temperature, time and deformation for a Si-Mn, a Nb and a Ti steel. Even at such high rolling temperatures, the niobium offers good resistance to grain growth compared to the Si-Mn steel; the Ti steel exhibits the highest resistance to grain growth due to the high solubility of the TiN precipitates in austenite.

The previous discussion concentrated mainly on Nb(CN) precipitates because they are believed to be the most effective and dominate precipitate system for inhibiting static recrystallization of austenite. However, the precipitate systems in Nb-Ti steels have been shown to have a more complex composition and morphology than the previously described Nb(CN) precipitate [Okaguchi and Hashimoto, 1987]. The transition metal carbides and nitrides possess a NaCl, B1 crystal structure making them mutually soluble. Thus, complex precipitates with a (Nb,Ti)(C,N) precipitate may form as well as complex particles consisting of a (Nb,Ti)(C,N) portion and a TiN or TiN-rich portion. At reheat temperatures around 2200°F (1200°C), the (Nb,Ti)(C,N) precipitates are cuboidal and Ti-rich and at lower reheat temperatures of around 1920°F (1050°C), the precipitates are spheroidal and Nb-rich. This phenomenon is attributed to the tendency for TiN to form in the liquid steel and at very high reheat temperatures and to the lower stability of Nb(CN) precipitates in austenite.

It was not within the scope of this study to characterize the nature of the precipitates (i.e. composition, size, volume fraction, distribution and proximity). Therefore, it is not known for certain the extent to which strain induced precipitation occurred or what precipitate species were present. However, some insight may be gained by considering the equilibrium thermodynamics of niobium carbonitride solubility in austenite. The solubility of a single metal/carbonitride precipitate may be expressed by the solubility product:

$$K = [M][C]^x[N]^y \quad [2]$$

where K = equilibrium solubility product,

[M], [C], and [N] = concentrations of metal (M), carbon (C) and nitrogen (N) in solid solution in equilibrium with the microalloy precipitate, MC_xN_y, and

x, y = the atomic ratio C/Nb and the atomic ratio N/Nb, respectively.

The solubility product can also be expressed as a function of temperature:

$$\text{Log } K = \text{Log } [M][C]^x[N]^y = A - B/T \quad [3]$$

where A and B are constants expressed such that the concentrations of the elements are in weight percent and T in °K. A recent review of the various solubility products for the Nb-C, Nb-N and Nb-C-N systems showed that several expressions have been derived to describe the solubility of the microalloy precipitate species [Palmiere et al., 1994]. The dissolution temperatures for Nb-C, Nb-N and Nb-C-N precipitate systems were calculated using the expressions summarized by Palmiere et al. and are shown in Table 2 using the carbon, niobium and nitrogen compositions from Table 1. Take note that the reheating temperature (2000°F (1093°C)) used during processing exceeded the average calculated dissolution temperatures for all of the precipitate systems. Therefore, it is highly probable that enough niobium, carbon, and nitrogen were in solution during processing to form strain induced precipitates.

With respect to the recrystallization study performed in this work, the suppression of recrystallization at 1650°F (900°C) at both 10% and 20% reductions after the first and second hits (Figures 6 and 7) was due to the pinning of austenite grain boundaries by Nb(CN) precipitates. However, Figure 7(a) shows that after three 20% hits and sixty second hold times, the steel begins to recrystallize due to the increase in kinetics resulting from the retained strain in the steel. For comparative purposes, Figure 16 shows the softening behavior of a Si-Mn steel deformed at various temperatures. The steel begins to recrystallize within ten seconds at 1472°F (800°C) and above. Figures 8(a) and 9(a) show the effects of increased temperature and strain on the recrystallization kinetics and it was observed that with 10% deformations, the pinning forces exerted by the Nb(CN) precipitates were sufficient to suppressed recrystallization at hold times less than twenty seconds; however, longer hold times led to recrystallization due to retained strain. Doubling the strain reduced

to ability of the Nb(CN) precipitates to retard the onset of recrystallization, especially after the second and third hits.

The effect of strain on the kinetics of static recrystallization is depicted in Figures 17 and 18 where the fraction of softening is plotted versus strain for each hold time. At 1650°F (900°C), all of the strain is retained[1] when 10% reductions are applied during each hit. When 20% reductions are employed, the strain is retained for all of the hold times except for 60 seconds where recrystallization begins after a true strain of 0.44. At 1800°F (982°C) and 10% reductions, strain is retained during all of the hold times shorter than 60 seconds. During the 60 second hold times, the steel began to recrystallize after a true strain of 0.2 was applied. When 20% reductions were applied at 1800°F (982°C), hold times less than 2 seconds are required to retain strain in the steel following deformation. Figure 18(b) shows that strain is no longer retained after the second hit (true strain = .44) for hold times between 2 and 20 seconds and after the first hit (true strain = 0.22) for the 60 second hold time.

The significance of the data presented in Figures 6 through 9 is that information regarding the static recrystallization kinetics derived from isothermal single and double hit compression tests should be coupled with multi-hit tests (three or more hits) to ascertain the effects of retained strain during controlled rolling. The results of this study indicated that the effects of retained strain are substantial and basing production rolling schedules on first pass kinetics alone may not be entirely accurate. For instance, double hit tests would indicate that the recrystallization stop temperature for HSLA-100 is around 1650°F (900°C) and for most cases this would be accurate, but at long hold times recrystallization may begin after several passes. Therefore, the effects of strain and time on the recrystallization stop temperature (T_{rxn}) should be thoroughly investigated to avoid undesirable microstructures such as the partially recrystallized microstructures observed in this study that result in bimodal grain size distributions. Bimodal grain sizes have been shown to be detrimental to the fracture toughness of HSLA steels [Tanaka, 1984, and Natishan, 1989]. Natishan showed that the critical stress for cleavage fracture is a function of the grain size and the grain size distribution such

[1]The retention of strain during deformation is inferred based on the suppression of static recrystallization and does not take static recovery into effect.

that a steel that has a microstructure that contains a fraction of large grains may fracture at a lower stress than a steel that exhibits a unimodal grain size distribution. The key to successful TMCP is to know the conditions under which full recrystallization occurs in a relatively short amount of time with limited grain growth for RCR and under which conditions recrystallization is fully suppressed for all levels of strain and hold times for CR.

CONCLUSIONS

The results of this study indicated that the static recrystallization kinetics of HSLA-100 were influenced by processing parameters. Static recrystallization was suppressed following hot deformation at 10% deformation per hit at 1650°F (900°C). At 1800°F (982°C), recrystallization began after the third hit and a sixty second hold time between each hit. Following 20% deformations per hit, the austenite began to recrystallize after three hits and a sixty second hold time between each hit at 1650°F (900°C). At 1800°F (982°C), the austenite began to recrystallize after the first hit and a sixty second hold time and the progress of recrystallization continued with each hit and with increasing hold time. The retardation of the austenite recrystallization kinetics was most likely due to the pinning of grain boundaries via the strain induced precipitation of niobium carbonitrides at the austenite substructure during deformation.

The information gained from the recrystallization study was used successfully to simulate recrystallization controlled rolling and a combination of recrystallization controlled rolling and controlled rolling. It was learned that hold times less than twenty seconds may result in partial recrystallization of austenite.

REFERENCES

Barbosa, R., Boratto, F., Yue, S., and Jonas, J.J., "The Influence of Chemical Composition on the Recrystallization Behavior of Microalloyed Steel," Proceedings of the International Symposium, Processing, Microstructure and Properties of HSLA Steels, A.J. DeArdo, Jr., Ed., TMS, Warrendale, PA, pp. 51-61, 1988.

Cuddy, L.J., Bauwn, J.J., and Raley, J.C., "Recrystallization of Austenite," *Metall. Trans.*, Vol 11A, pp 381-386, 1980.

DeArdo, A.J., Gray, J.M., and Meyer, L., "Fundamental Metallurgy of Niobium in Steel," Proceedings of the International Symposium, Niobium '81, AIME, N.Y., N.Y., pp 685-760, 1984.

DeArdo, A.J., "Fundamental Aspects of the Physical Metallurgy of Thermomechanical Processing of Steel," International Conference on Physical Metallurgy of Thermomechanical Processing of Steels and Other Metals, Japan, ISI, p 20, 1988.

DeArdo, A.J., "Accelerated Cooling: A Physical Metallurgy Perspective," *Can. Metall. Quart.*, Vol 27, No. 2, pp 141-154, 1988.

Djaic, R.A.P., and Jonas, J.J., "Recrystallization of High Carbon Steel Between Intervals of High Temperature Deformation," *Metall. Trans.*, Vol. 4A, pp 621-625, 1973.

Hamburg, E.G., and Wilson, A.D., "Production and Properties of Copper Age Hardened Steels," Proceedings of the International Symposium, Processing, Microstructure and Properties of HSLA Steels, TMS, Warrendale, PA, pp 241-260, 1988.

Hansen, S.S., Vander Sande, J.B., and Cohen, M., "Niobium Carbonitride Precipitation and Austenite Recrystallization in Hot-Rolled Microalloyed Steels," *Metall. Trans.*, Vol. 11A, pp 387-402, 1980.

Kwon, O.J., PhD. Thesis, University of Pittsburgh, 1985.

Kwon, O.J., and DeArdo, A.J., "Niobium Carbonitride Precipitation and Static Softening in Hot Deformed Niobium Microalloyed Steels," HSLA Steels: Metallurgy and Applications, J.M. Gray, T. Ko, Z. Shouhua, B. Wu, X. Xie, Eds., ASM, Metals Park, OH, pp 287- , 1986.

Kwon, O.J., and DeArdo, A.J., "Interactions Between Recrystallization and Precipitation in Hot-Deformed Microalloyed Steels," *Acta Metall. Mater.*, Vol 39, No. 4, pp 529-538, 1991.

Laasraoui, A. and Jonas, J.J., "Recrystallization of Austenite After Deformation at High Temperatures and Strain Rates - Analysis and Modeling," *Metall. Trans.*, Vol 22A, pp 151-160, 1991.

Natishan, M.E., "Mechanisms of Strength and Toughness in a Microalloyed, Precipitation Hardened Steel," DTRC Report: SME-88-81, April 1989.

Okaguchi, S. and Hashimoto, T., "Characteristics of Precipitates and Mechanical Properties in Ti Bearing HSLA Steels," *Transactions ISIJ*, Vol. 27, pp 467-472.

Ouchi, C., Sampei, T., Okita, T., and Kozasu, I., "Microstructural Changes of Austenite During Hot Rolling and Their Effects on Transformation Kinetics," Hot Deformation of Austenite, J. Ballance, Ed., TMS-AIME, New York, p 316, 1976.

Ouchi, C., "Softening Behavior Immediately After Rolling and Strain Accumulation," in: Thermomechanical Processing of High Strength Low Alloy Steels, I. Tamura, C. Ouchi, T. Tanaka, H. Sekine, Eds., Ch. 7, pp 128-139, 1988.

Palmiere, E.J., Garcia, C.I., and DeArdo, A.J., "Composition and Microstructural Changes Which Attend Reheating and Grain Coarsening in Steels Containing Niobium," *Metall. Trans.*, Vol. 25A, pp 277-286, 1994.

Sekine, H., and Maruyama, T. The Microstructure and Design of Alloys, The Metals Society, Vol I, p 85, 1973.

Simoneau, R., Begin, G., and Marquis, A.H., "Progress of Nb(CN) Precipitation in HSLA Steels as Determined by Electrical Resistivity Measurements," *Met. Sci.*, Vol. 12, pp 381-386, 1978.

Tanaka, T., "Four Stages of Thermomechanical Processing in HSLA Steel" TMS-AIME Conference Proceedings on High Strength Low Alloy Steels, D.P. Dunne and T. Chandra, Eds., pp. 6-16, 1984.

Thompson, S.W., Colvin, D.J. and Krauss, G., "Continuous Cooling Transformation and Microstructures in a Low-Carbon, High-Strength Low-Alloy Plate Steel," *Metall. Trans.*, Vol 21A, pp 1493-1507, 1990.

Wilson, A.D., Hamberg, E.G., Colvin, D.J., Thompson, S.W. and Krauss, G., "Properties and Microstructure of Copper Precipitation Aged Plate Steels," Proceedings of Microalloying '88, World Materials Congress, ASM, Metals Park, OH, 1988.

Yamamoto, S., Ouchi, C. and Osuka, T., "The Effect of Microalloying Elements on the Recovery and Recrystallization in Deformed Austenite," Proceedings of the International Conference, Thermomechanical Processing of Microalloyed Austenite, A.J. DeArdo, G.A. Ratz, P.J. Wray, Eds., AIME, Warrendale, PA, pp 613-639, 1982.

Yoshie, A., Morikawa, H., Onoe, Y., and Itoh, K., "Formulation of Static Recrystallization of Austenite in Hot Rolling Process of Steel Plate," *Trans. ISIJ*, Vol. 27, pp 425-431, 1987.

Table 1 Chemical Composition of HSLA-100 Slab Material

Element (weight %)	Chemical Composition	
	HSLA-100 MIL-S-24645A (maximum unless range is shown)	HSLA-100 Slab (GSP)
C	0.06	0.040
Mn	0.75-1.05	0.84
P	0.020	0.005
S	0.006	0.002
Cu	1.45-1.75	1.61
Si	0.400	0.32
Ni	3.35-3.65	3.49
Cr	0.45-0.75	0.56
Mo	0.55-0.65	0.61
Ti	0.020	0.015
Nb	0.02-0.06	0.031

Table 2 Dissolution Temperatures of Various Carbonitride Precipitate Species Based On Equilibrium Solubility Equations [Palmeire, 1994]

Carbonitride Species	Equilibrium Dissolution Temperature	
	°F	°C
Nb-C	1862	997
Nb-$C_{0.87}$	1819	993
Nb-C-N	1915	1046
Nb-N	1951	1066

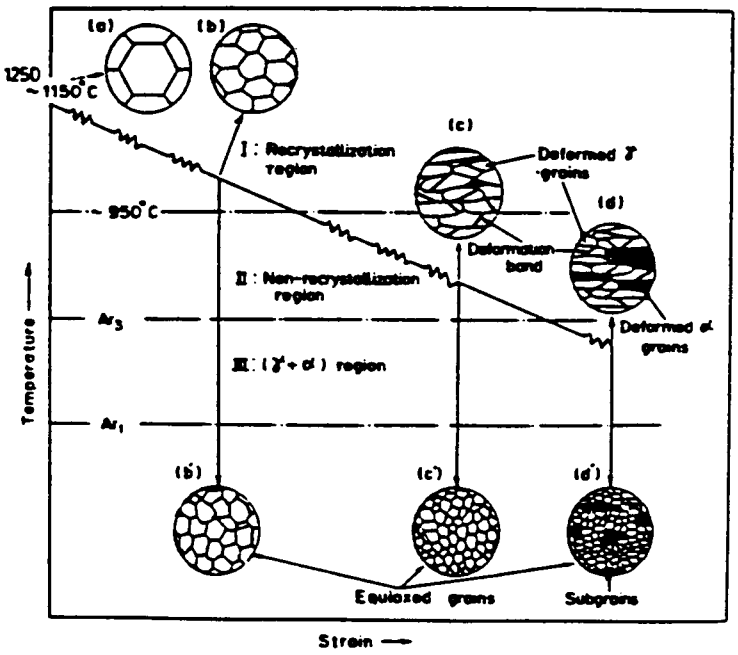

Figure 1 The four stages of thermomechanical processing [Tanaka, 1984]

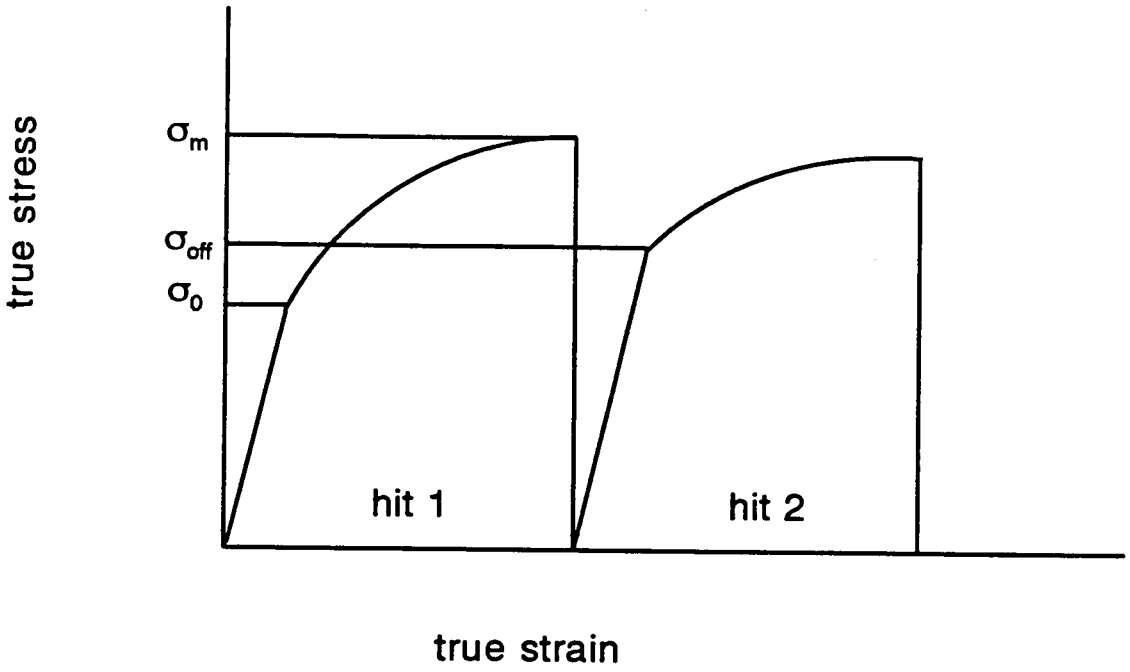

Figure 2 Schematic illustration of true stress/true strain curves obtained to measure static softening during multi-hit deformation tests.

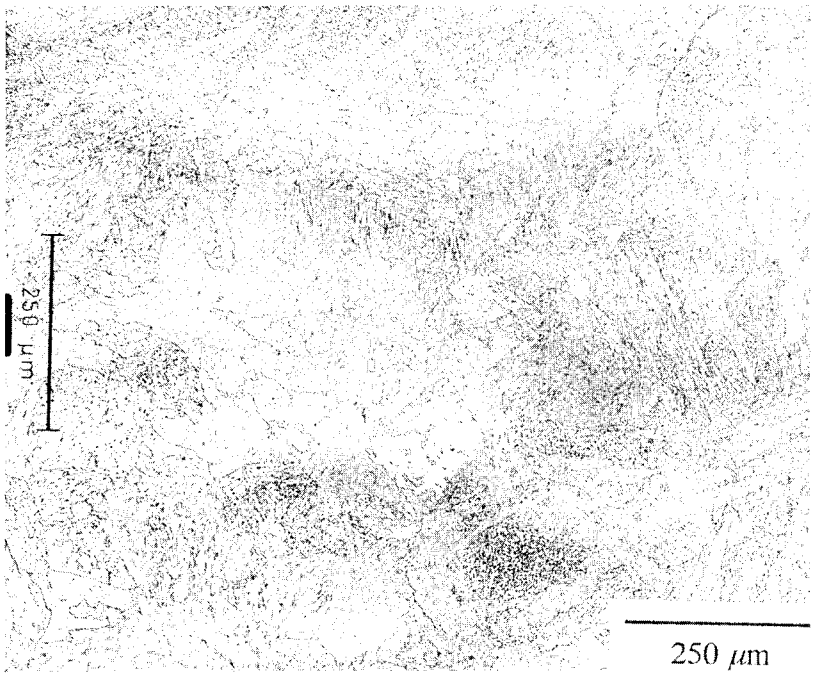

Figure 3 Microstructure of HSLA-100 in the as-slabbed condition.

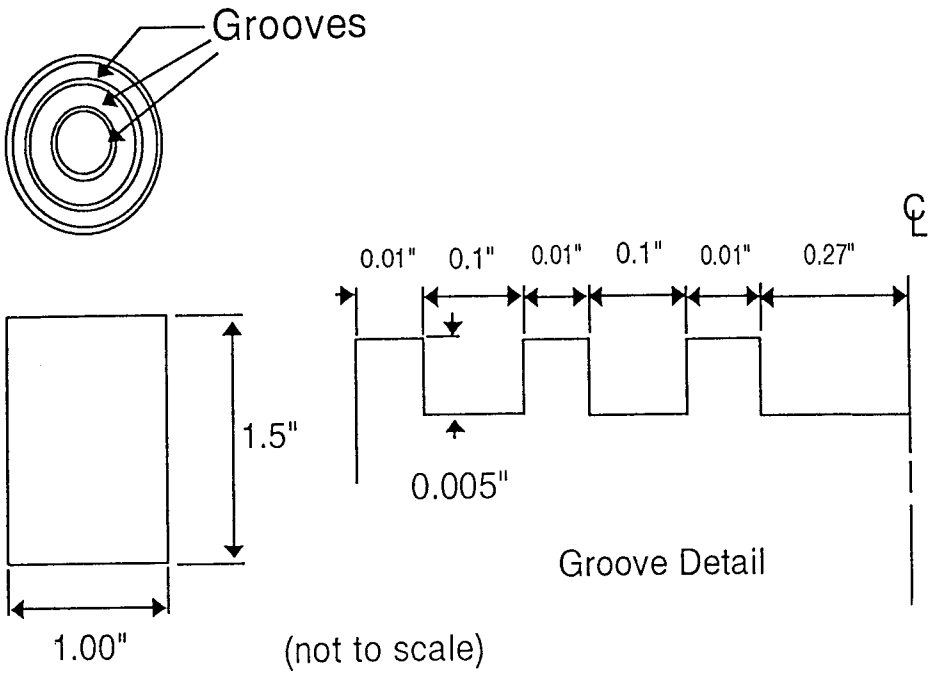

Figure 4 Schematic illustration of the TMCP specimen.

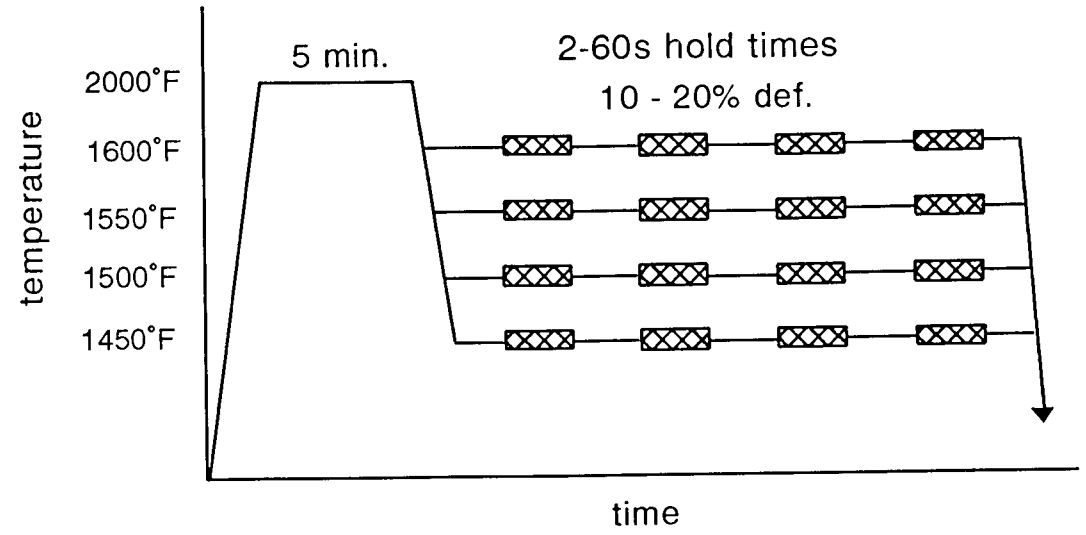

(a)

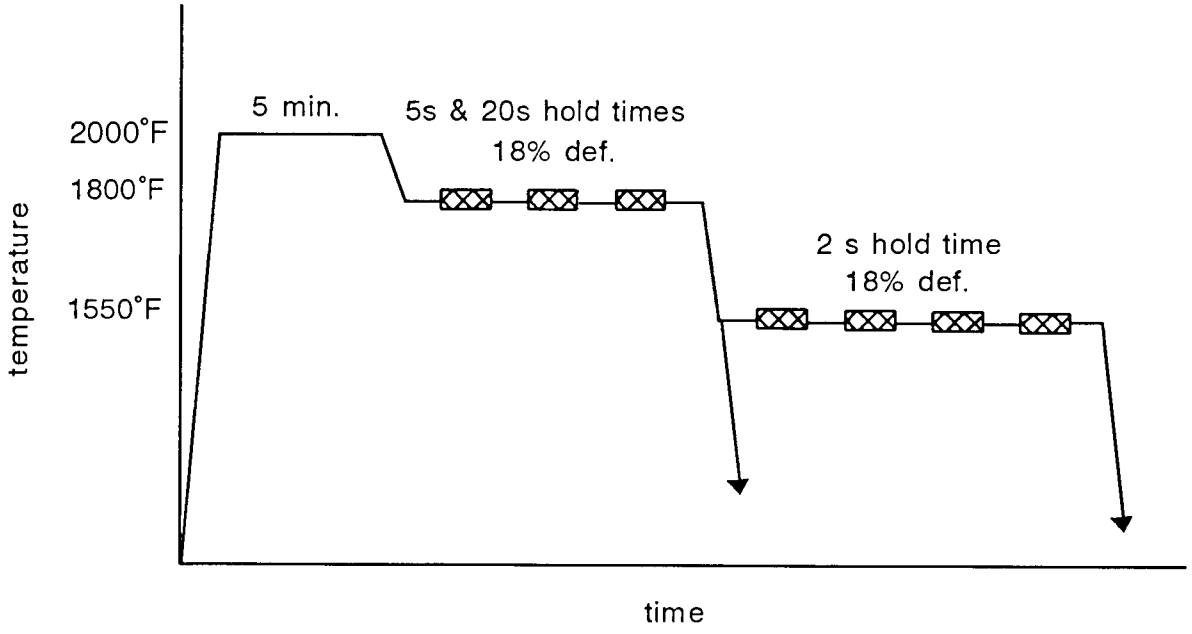

(b)

Figure 5 Schematic illustration of processing routes for (a) the recrystallization study and (b) the RCR and RCR + CR simulations.

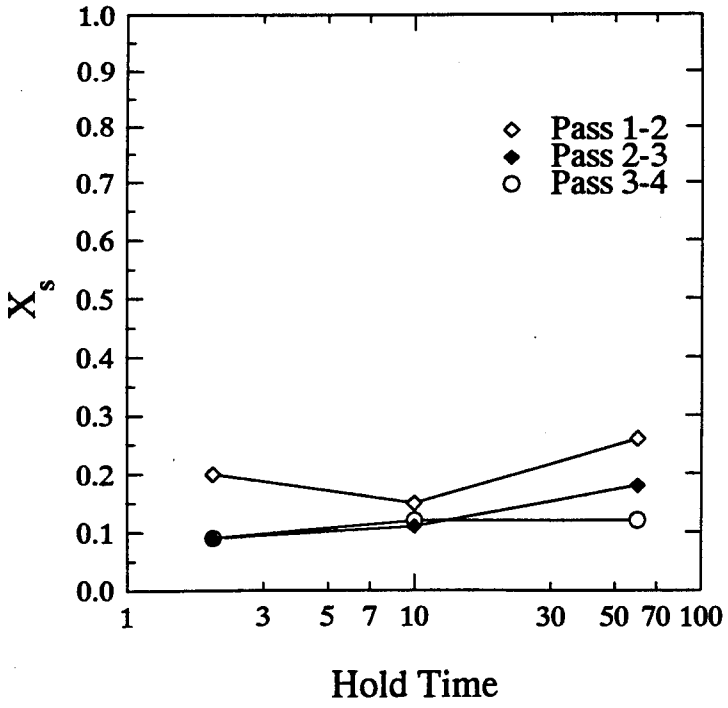

(a)

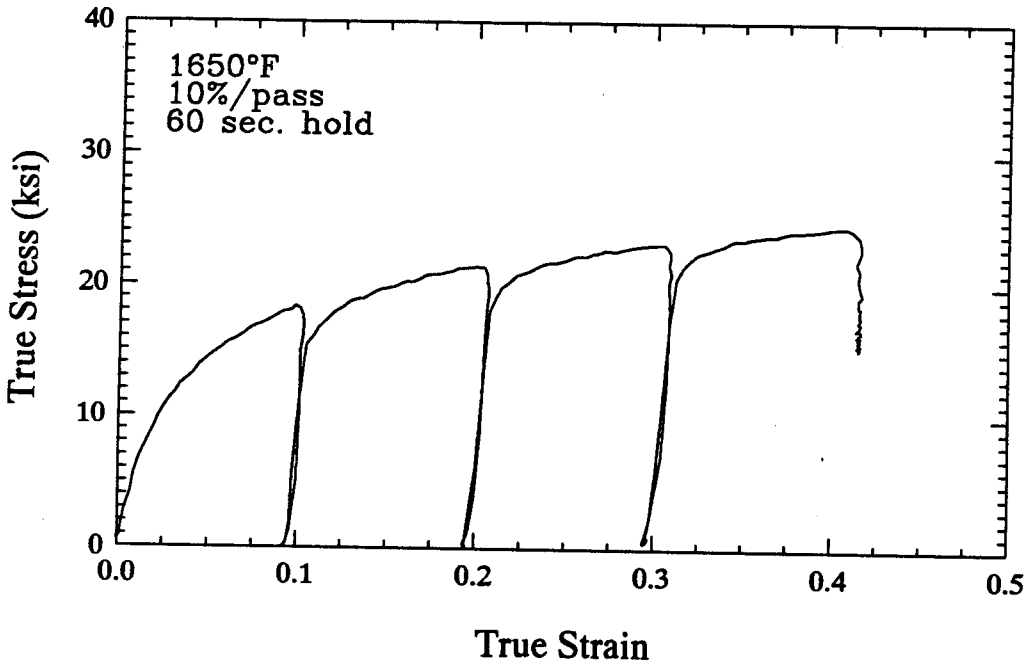

(b)

Figure 6 (a) Fractional softening vs. hold time for HSLA-100 deformed at 900°C (1650°F) and 10% deformation, and (b) the corresponding true stress/true strain curves for the 60 second hold time.

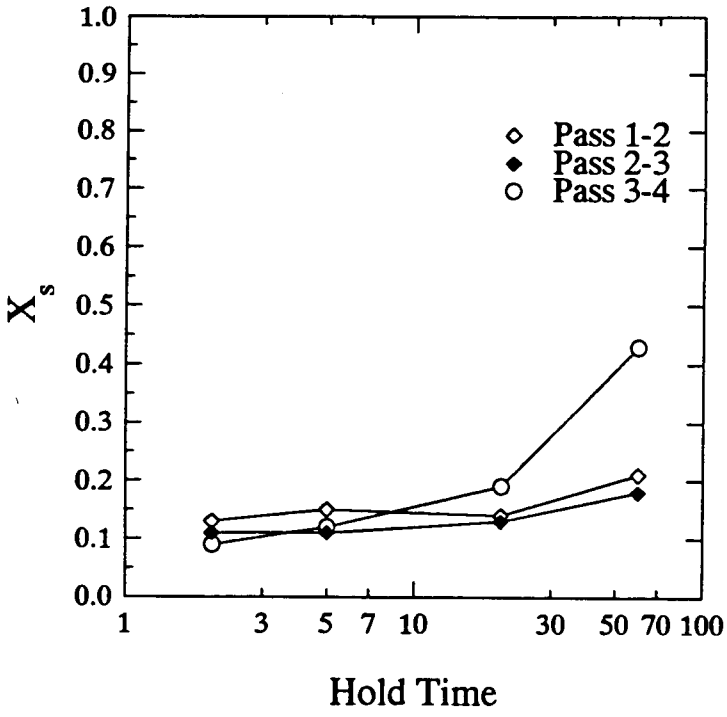

(a)

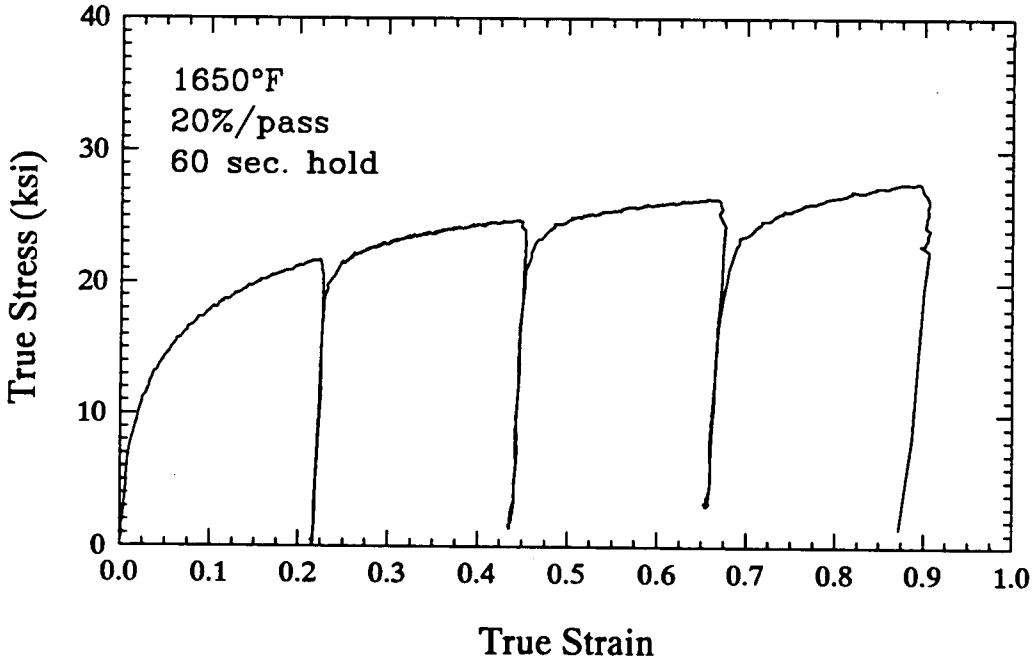

(b)

Figure 7 (a) Fractional softening vs. hold time for HSLA-100 deformed at 900°C (1650°F) and 20% deformation, and (b) the corresponding true stress/true strain curves for the 60 second hold time.

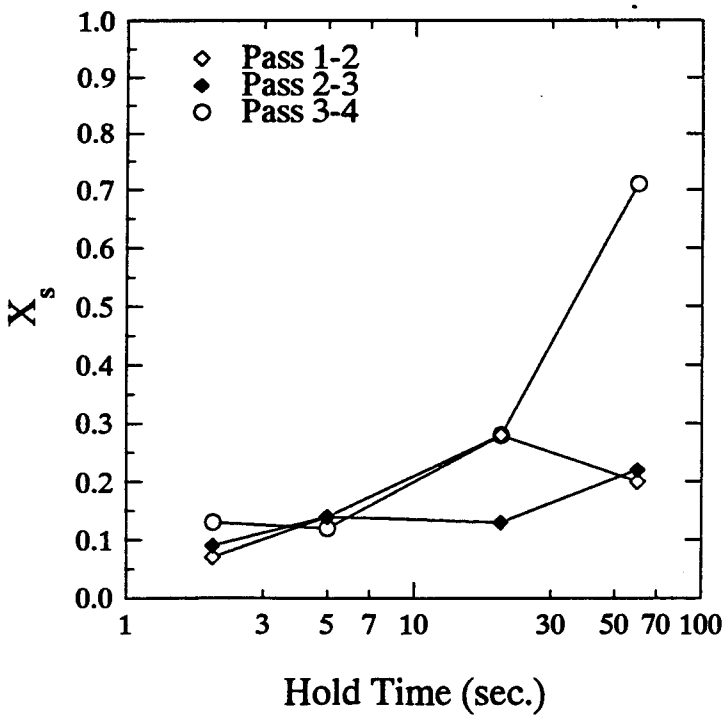

(a)

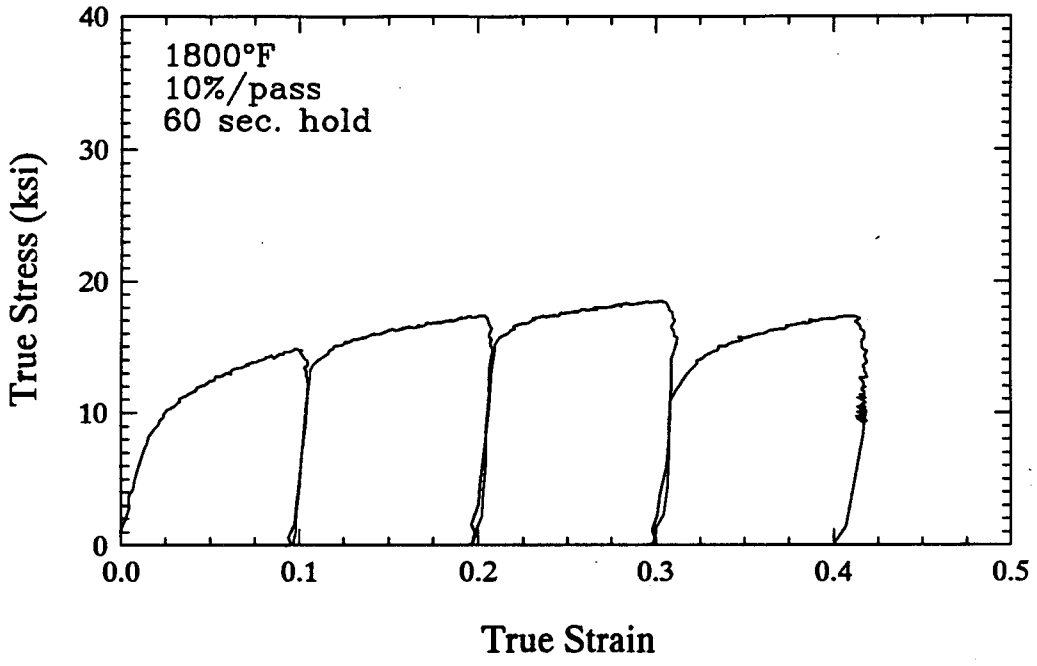

(b)

Figure 8 (a) Fractional softening vs. hold time for HSLA-100 deformed at 982°C (1800°F) and 10% deformation, and (b) the corresponding true stress/true strain curves for the 60 second hold time.

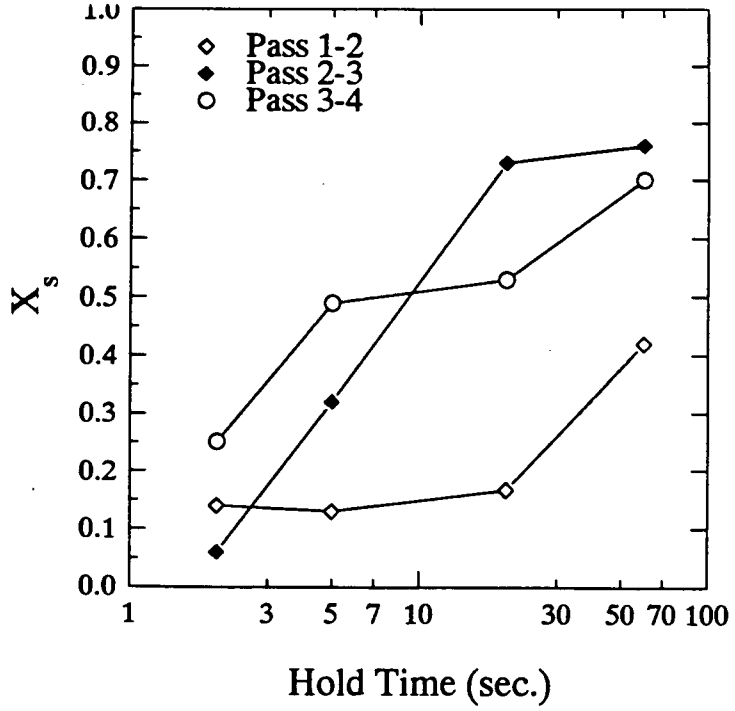

(a)

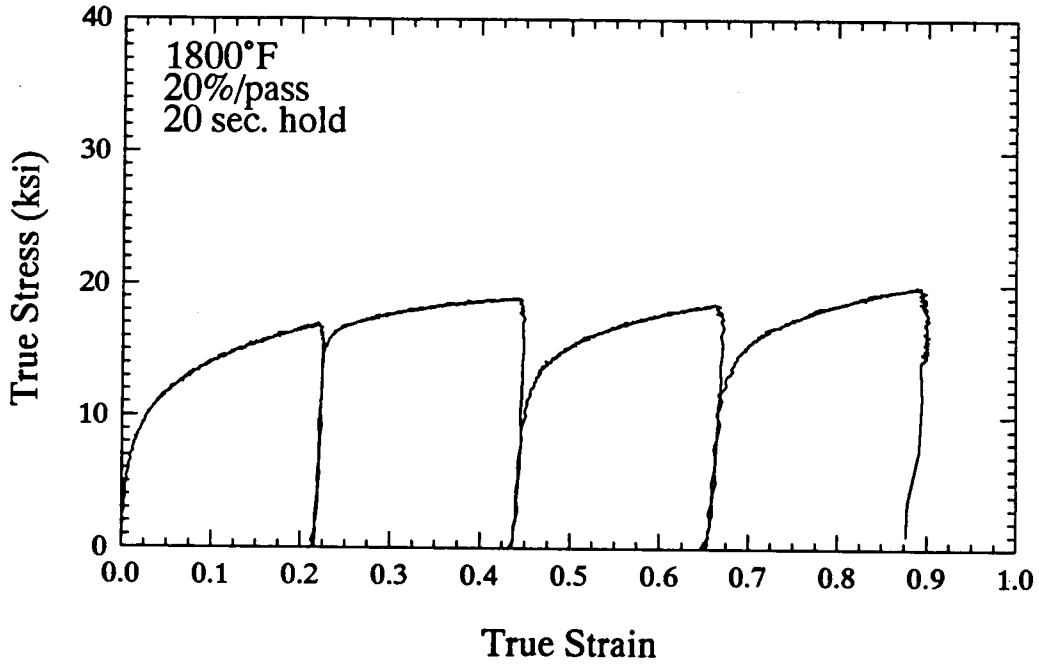

(b)

Figure 9 (a) Fractional softening vs. hold time for HSLA-100 deformed at 982°C (1800°F) and 20% deformation, and (b) the corresponding true stress/true strain curves for the 20 second hold time.

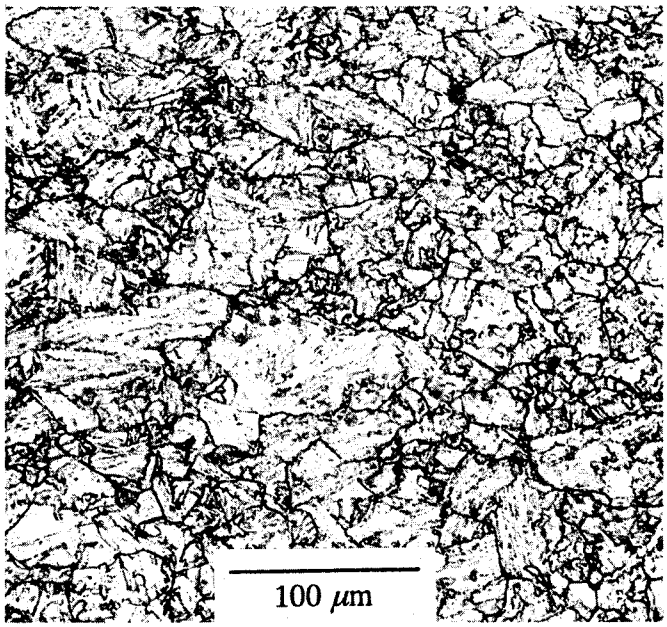

20% def./hit, 3 hits, 5 sec. hold times
g.s. = 19 μm

(a)

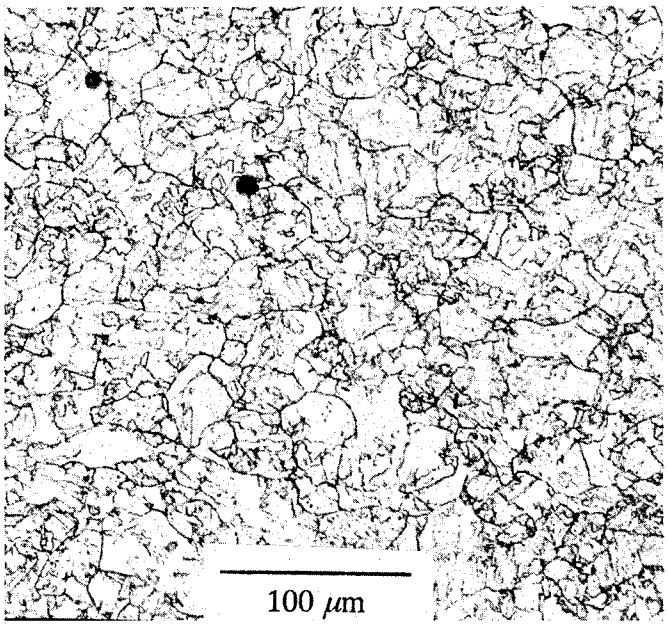

20% def/hit., 3 hits, 20 sec. hold times
g.s. = 22 μm

(b)

Figure 10 Microstructures of HSLA-100 subjected to (a-d) RCR processing at 1800°F (982°C) and different hold times, strains and number of hits and (e) RCR at 1800°F (982°C) + CR at 1550°F (982°C).

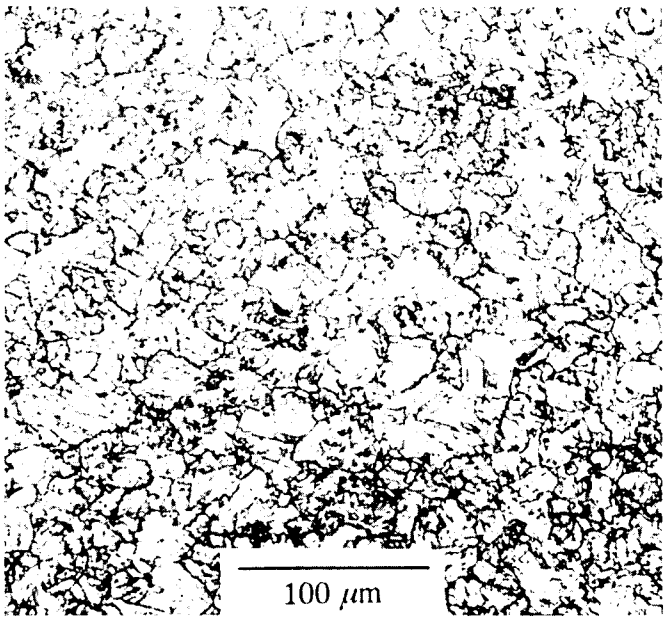

20% def./hit, 6 hits, 5 sec. hold times
g.s. = 20 μm

(c)

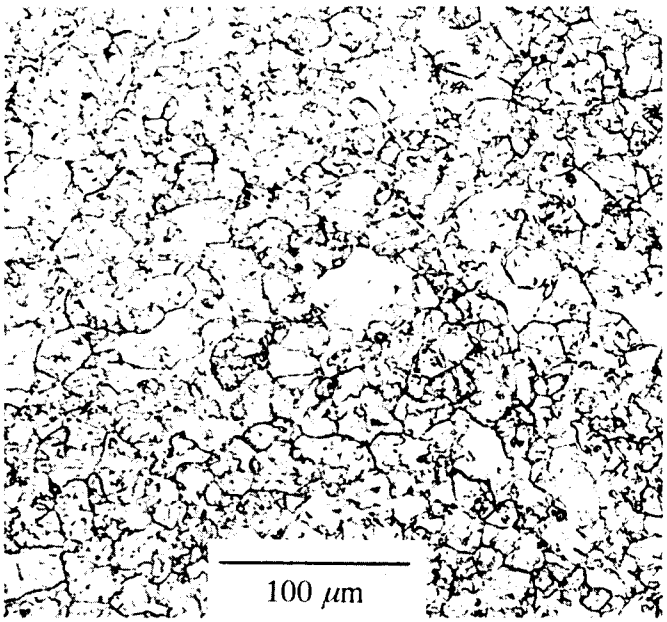

20% def./hit, 6 hits, 20 sec. hold times
g.s. = 21 μm

(d)

Figure 10 (cont.) Microstructures of HSLA-100 subjected to (a-d) RCR processing at 1800°F (982°C) and different hold times, strains and number of hits and (e) RCR at 1800°F (982°C) + CR at 1550°F (982°C)

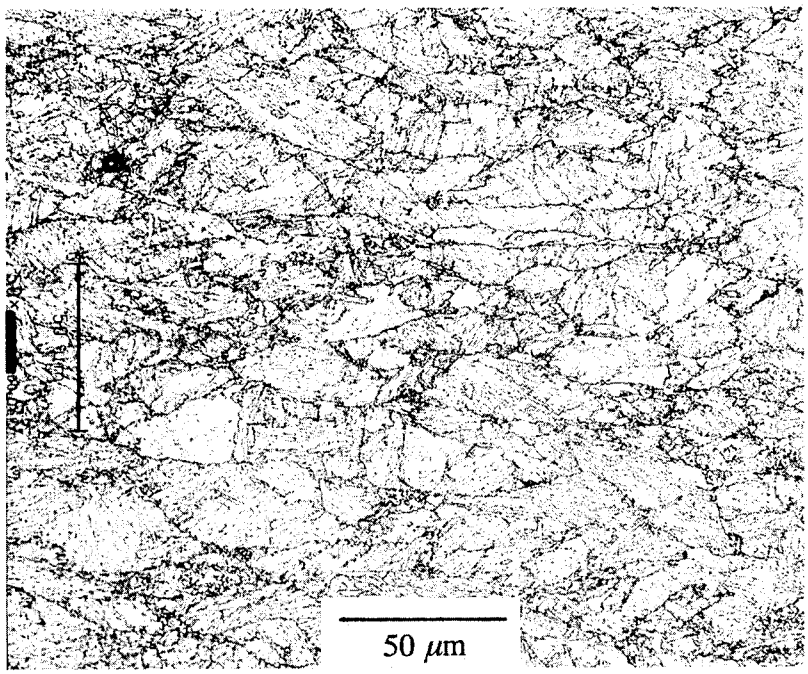

RCR: 18% def./hit, 3 hits, 20 sec. hold times

CR: 18% def./hit, 4 hits, 2 sec. hold times
PAG thickness = 15 μm
(e)

Figure 10 (cont.) Microstructures of HSLA-100 subjected to (a-d) RCR processing at 1800°F (982°C) and different hold times, strains and number of hits and (e) RCR at 1800°F (982°C) + CR at 1550°F (982°C)

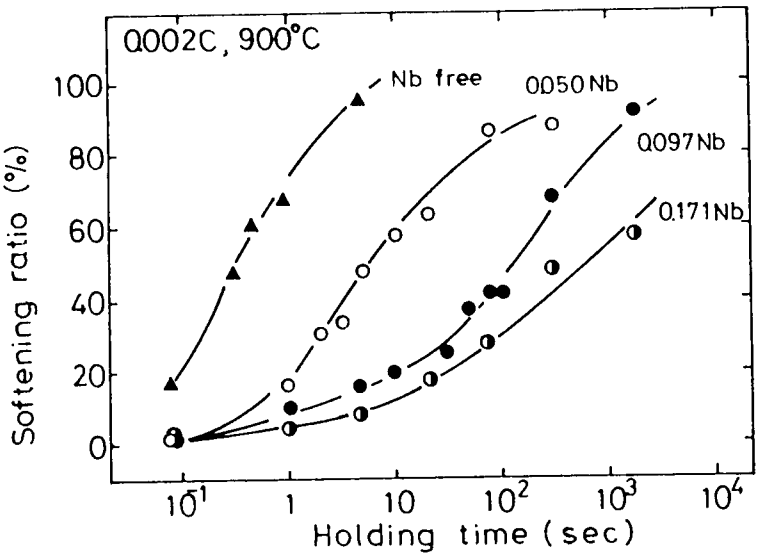

(a)

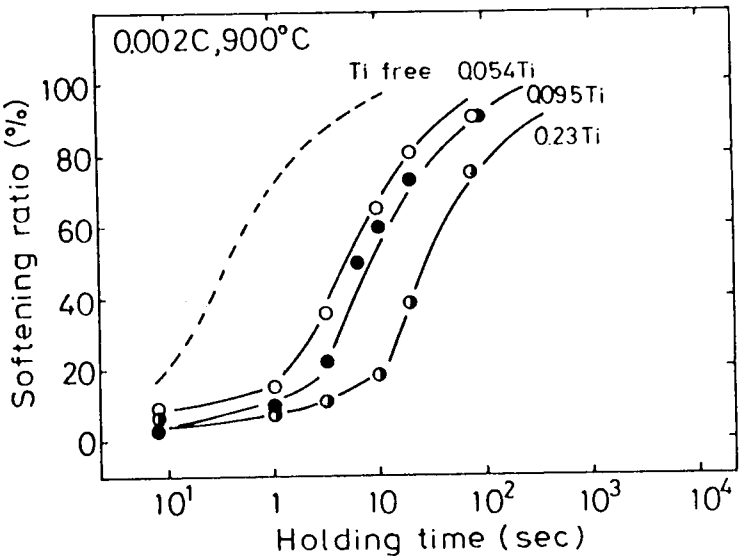

(b)

Figure 11 The softening behavior of various (a) Nb steels and (b) Ti steels with 0.002% C. These curves illustrate the effect of Nb and Ti in solution in austenite at the deformation temperature. [Yamamoto et al. 1982]

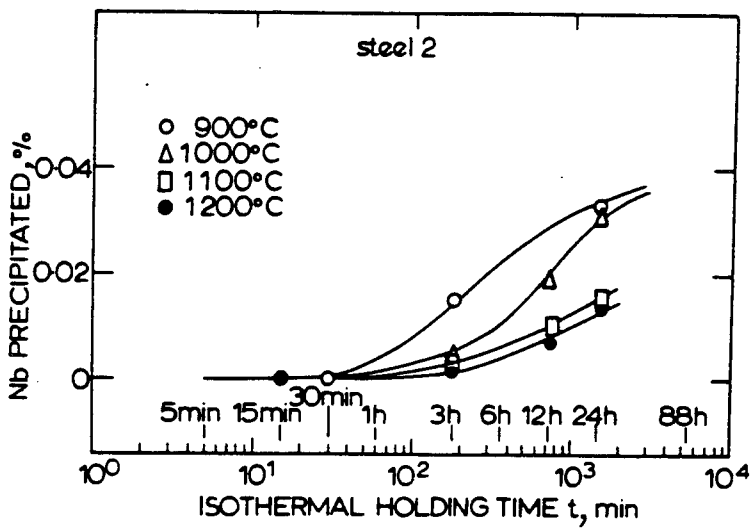

Figure 12 Isothermal precipitation of Nb in undeformed austenite in a 0.07% C, 0.04% Nb, 0.01% N steel. [Simoneau et al., 1978]

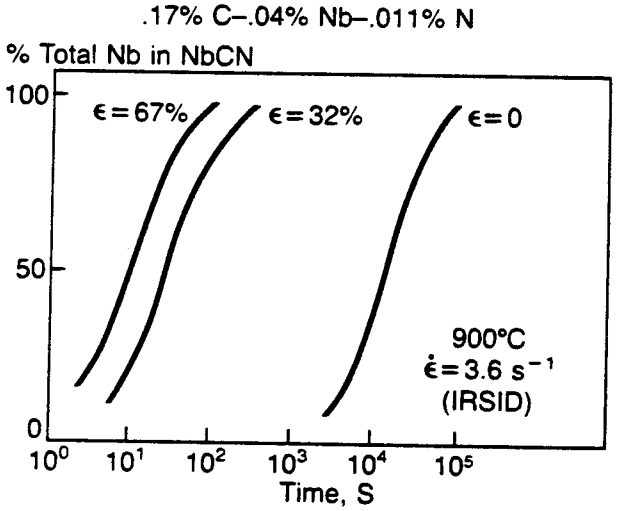

Figure 13 Influence of strain level on the kinetics of Nb precipitation at 900°C (1650°F). [DeArdo, 1984]

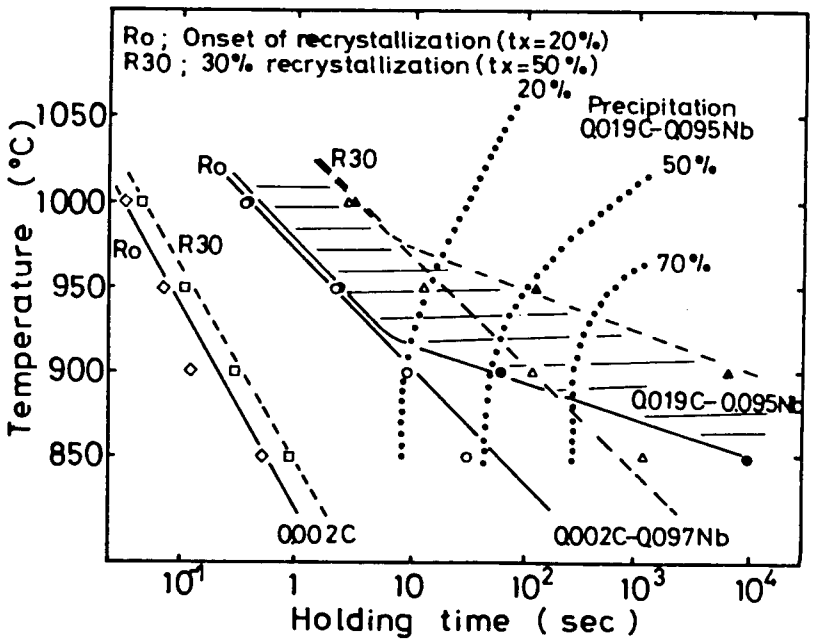

Figure 14 Recrystallization-precipitation diagram for C-Mn and C-Mn-Nb steels. [Yamamoto et al., 1982]

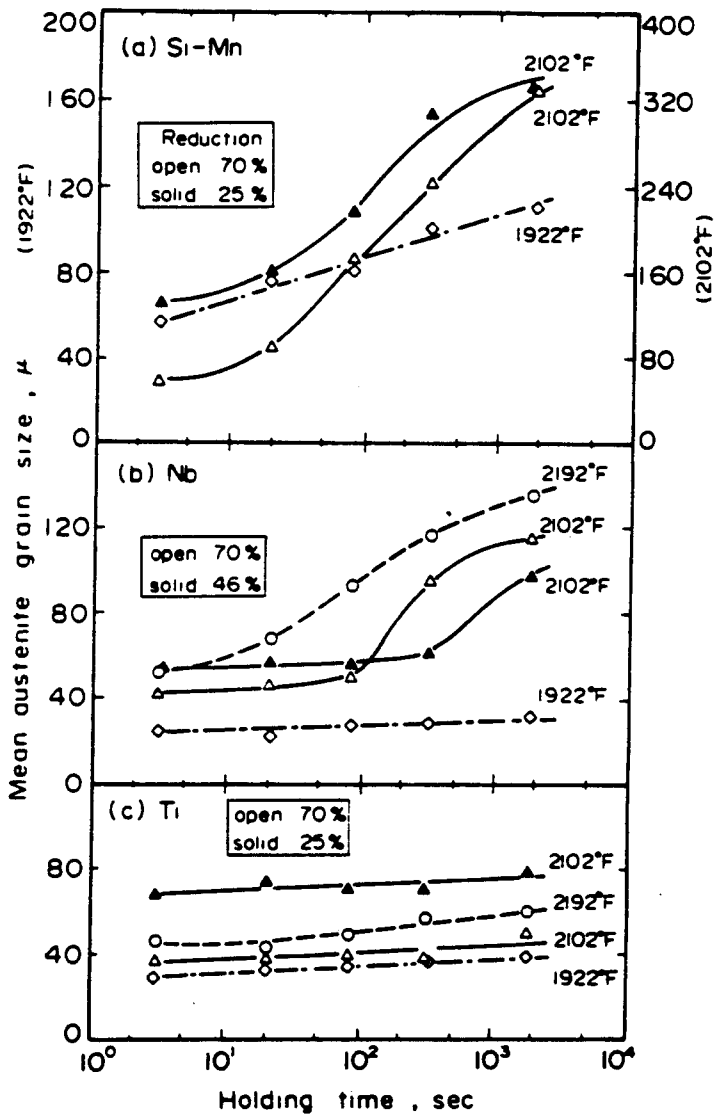

Figure 15 Grain growth behavior after hot rolling (a) Si-Mn steel (b) Nb steel and (c) Ti steel. [Ouchi et al., 1976]

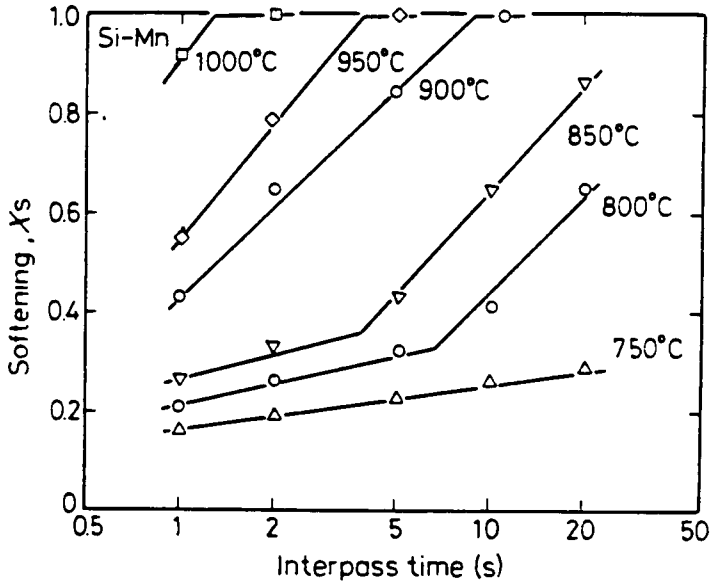

Figure 16 Effect of interpass time and deformation temperature on the softening ratio: Si-Mn steel, prestrain 0.2. [Ouchi et al., 1988]

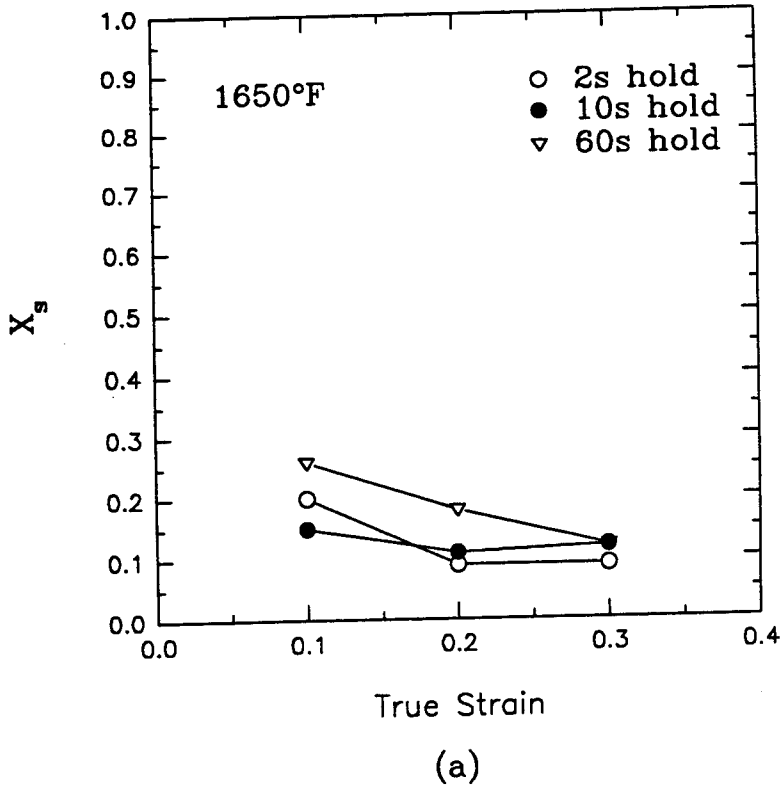

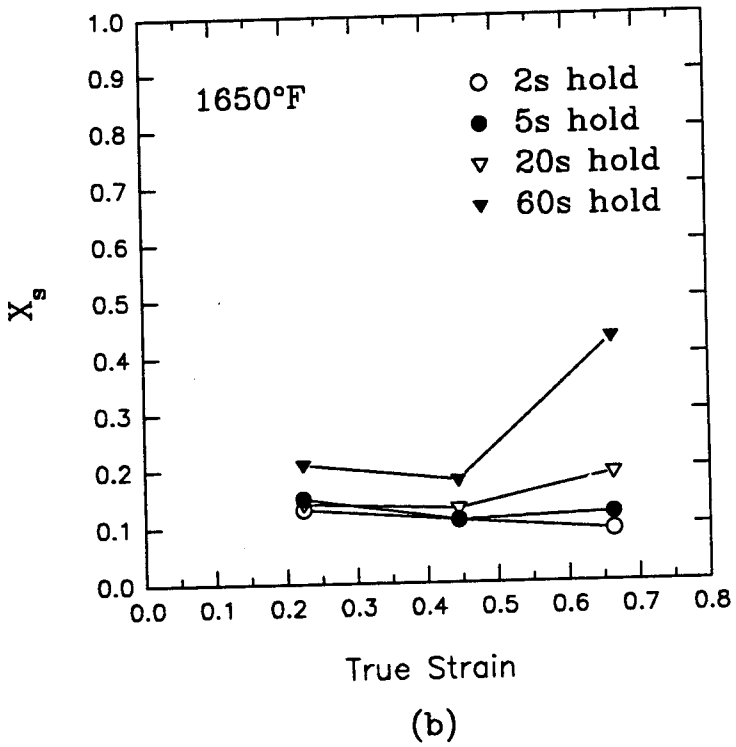

Figure 17 Fraction of softening vs true strain for deformation tests performed at 1650°F (900°C) with (a) 10% deformation per hit and (b) 20% deformation per hit.

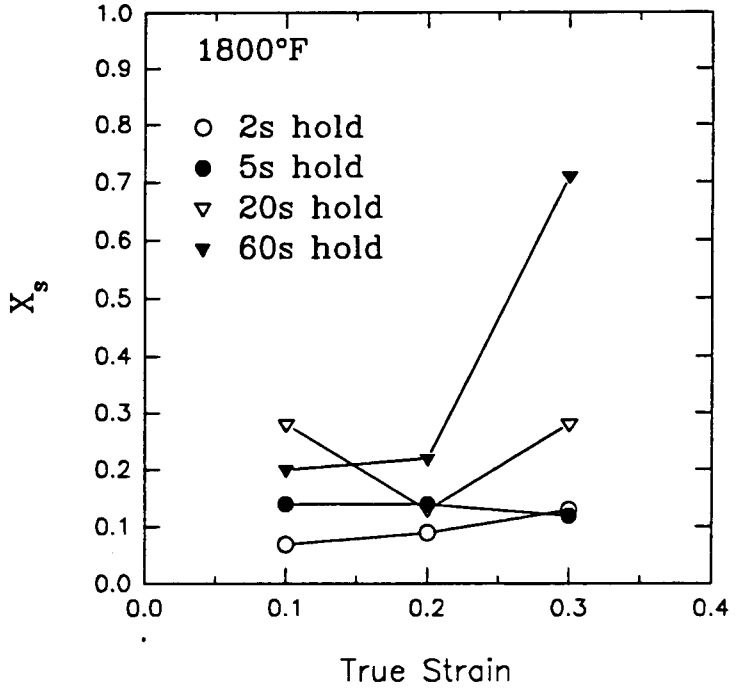

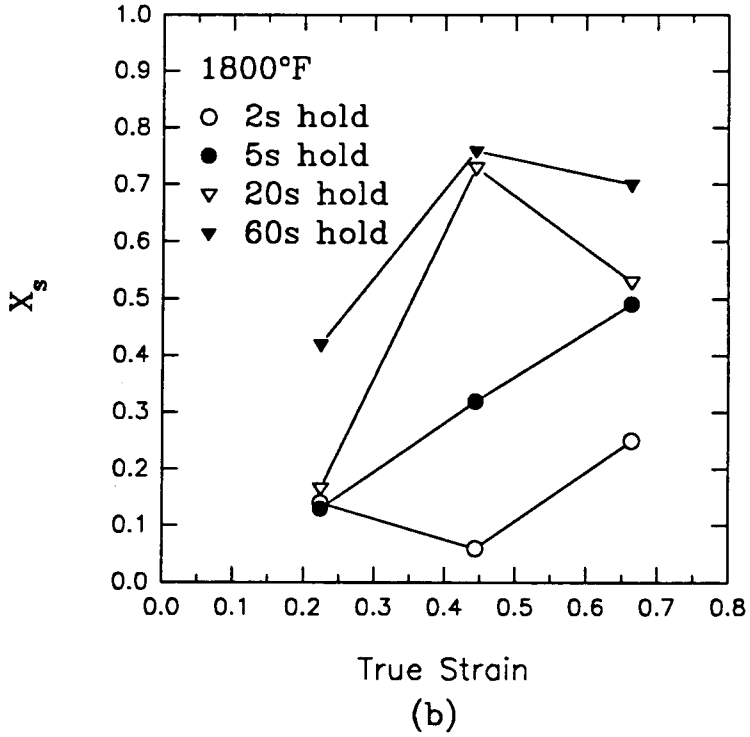

Figure 18 Fraction of softening vs true strain for deformation tests performed at 1800°F (982°C) with (a) 10% deformation per hit and (b) 20% deformation per hit.

INITIAL DISTRIBUTION

Copies

3 OCNR
- 1 0332
- 1 0332 (Sloter)
- 1 0332 (Vasudivan)
- 1 Library

18 NAVSEA
- 1 SEA 03M
- 5 SEA 03M2
- 1 SEA 03P4 (Manuel)
- 1 SEA 03R
- 1 SEA 393T

1 FHWA (Wright)

4 DTIC

1 NAVPGSCOL

1 USNROTCU
NAVAMINU MIT

2 NRL
- 1 Code 6326
- 1 Code 6382

1 Title III Program Office,
AFSC/PLMM (W. Johnson)

DIVISION DISTRIBUTION

Copies	Code
1	0115
2	2033
1	60
1	603
1	61
1	61s
1	61.1
1	612
1	613
1	614
10	614 (EMF)
1	614 (EJC)
1	614 (RLJ)
1	614 (WCP)
1	614 (RLT)
1	614 (CR)
1	614 (REL)
1	614 (WW)
1	615 (MGV)
1	62
1	623
1	625
1	65
1	65.1
1	65.2
1	65.3
1	66
1	66.3
1	67
1	68
1	322.1
1	322.2
2	3231